AIP | Review of Scientific Instruments

Density fluctuation measurements by far-forward collective scattering in the MST reversed-field pinch

W. X. Ding, L. Lin, J. R. Duff, D. L. Brower, and J. S. Sarff

Citation: Rev. Sci. Instrum. **83**, 10E302 (2012); doi: 10.1063/1.4728098
View online: http://dx.doi.org/10.1063/1.4728098
View Table of Contents: http://rsi.aip.org/resource/1/RSINAK/v83/i10
Published by the American Institute of Physics.

Density fluctuation measurements by far-forward collective scattering in the MST reversed-field pinch[a)]

W. X. Ding,[1] L. Lin,[1,b)] J. R. Duff,[2] D. L. Brower,[1] and J. S. Sarff[2]
[1]*Department of Physics and Astronomy, University of California Los Angeles, Los Angeles, California 90095, USA*
[2]*Department of Physics, University of Wisconsin–Madison, Madison, Wisconsin 53706, USA*

(Presented 8 May 2012; received 7 May 2012; accepted 23 May 2012; published online 6 June 2012)

The multichannel polarimeter-interferometer system on the MST reversed-field pinch can be utilized to measure far-forward collective scattering from electron density fluctuations. The collective scattering system has 11 viewing chords with ~8 cm spacing. The source is a 432 μm (694 GHz) far infrared laser and the scattered power is measured using a heterodyne detection scheme. Collective scattering provides a line-integrated measurement of fluctuations within the divergence of the probe beam covering wavenumber range: $k_\perp < 1.3$ cm^{-1}, corresponding $k_\perp \rho_s < 1.3$ (ρ_s is the ion-sound Larmor radius), the region of primary interest for turbulent fluctuation-induced transport. The perpendicular wavenumber consists of toroidal, poloidal, and radial contributions, which vary with chord position. Coherent modes associated with tearing instabilities and neutral-beam driven fast particles are observed along with broadband turbulence at frequencies up to 500 kHz. Changes in frequency are consistent with a Doppler shift due to parallel plasma flow. © *2012 American Institute of Physics*. [http://dx.doi.org/10.1063/1.4728098]

I. INTRODUCTION

Understanding fluctuation-induced particle and thermal transport in fusion plasmas requires a joint theoretical and experimental effort.[1] In the reversed-field pinch (RFP) community, large-scale magnetohydrodynamics (MHD) instabilities have been extensively explored experimentally and theoretically, and are generally believed to be responsible for dynamo generation along with particle and thermal transport in standard sawtoothing RFP plasmas. Microturbulence had not drawn much attention until the advent of high-performance RFP plasmas where large-scale MHD instability-induced transport is greatly reduced by manipulating the current density distribution. These high-performance plasmas are achieved either through externally added pulsed poloidal current drive (PPCD),[2] or through the spontaneous evolution of RFP plasmas at high plasma current.[3,4] Numerical simulations of these improved confinement plasmas indicate that unstable ion temperature gradient (ITG)[5,6] and micro-tearing modes[7] may dominate the transport. In addition, RFP plasmas heated by neutral beam injection (NBI) show the evidence of narrowband fast-particle instabilities that can effect energetic ion confinement. Predictions related to these effects motivate the need for the measurements of both coherent and broadband turbulent fluctuations in RFPs for the purpose of validating numerical predictions and understanding the physics of confinement.

The multichannel polarimeter-interferometer system on MST-RFP (Refs. 8 and 9) can be exploited to simultaneously measure far-forward collective scattering resulting from electron density fluctuations. This technique has successively measured coherent modes associated with tearing modes, neutral-beam driven instabilities, and broadband turbulence up to 500 kHz. In this paper, we describe the system along with these results.

II. FAR-FORWARD SCATTERING

The optical scheme of the far-forward collective scattering system on MST is shown in Fig. 1. Two far infrared (FIR) 432 μm (694 GHz) lasers (ω_1 and ω_2) are frequency offset ~1 MHz to permit heterodyne detection. For simplicity, only 1 of the 11 probe beams is shown in Fig. 1. Along the same sightlines and using the same FIR beams, interferometry and Faraday-rotation polarimetry are also made.[8] In the real system on MST, the laser ω_1 is divided into 12 parts: 11 probe beams and one reference beam. These 11 beams pass vertically through the plasma at impact parameters: $x = R - R_0 = -0.24, -0.09, 0.06, 0.21, 0.36$ m located at toroidal angle 250° and $-0.32, -0.17, -0.02, 0.13, 0.28, 0.43$ m located at toroidal angle 255°. The 5° toroidal offset can be used to gain information on the fluctuation wavenumber spectrum (as will be discussed later). The laser ω_2 serves as the local oscillator and is also divided into 12 parts to provide the RF bias for the 12 Schottky-diode corner-cube mixers (11 for probe beam and one for reference beam). The signals from the mixers are digitized at 6 MHz. The reference beam is not necessary for the scattering system but permits the simultaneous operation of the heterodyne interferometry (and polarimetry if a third laser beam is employed). Phase comparison of probe beams and reference beam gives the line-integrated density. All the experiments reported here are performed on the MST,[10] a toroidal reversed field pinch device with minor radius a = 0.5 m and major radius $R_0 = 1.5$ m.

[a)]Contributed paper, published as part of the Proceedings of the 19th Topical Conference on High-Temperature Plasma Diagnostics, Monterey, California, May 2012.

[b)]Author to whom correspondence should be addressed. Electronic mail: lianglin@ucla.edu.

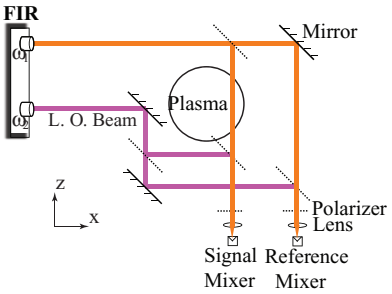

FIG. 1. Optical scheme of heterodyne far-forward scattering system. For simplicity, only one of the 11 probe beams is shown. The reference beam is also shown, which permits a simultaneous operation of a heterodyne interferometry system.

A collective scattering system[11–13] measures the scattered power due to electron density fluctuations. Scattered power (P_s) is proportional to the square of the density fluctuation amplitude ($\tilde{n}^2$), i.e., $P_s \propto \tilde{n}^2$. Maximum $k_\perp$ (wavenumber perpendicular to probe beam) sensitivity is determined by the beam width (w). For the system on MST, the beam width is ~2.5 cm in the plasma, giving $k_\perp \leq \pi/w \sim 1.3\ \text{cm}^{-1}$. For typical plasma parameters (electron temperature $T_e \sim 400$ eV and magnetic field $B \sim 0.3$ T), this maximum $k_\perp$ corresponds to $k_\perp \rho_s \leq 1.3$, where ρ_s is the ion-sound Larmor radius. This makes the MST far-forward scattering system sufficient for detecting both the ITG and micro-tearing modes. No modification of the polarimetry-interferometry system is required to access the collective scattering information. However, if desired, modifying the light collection optics would allow for the detection of even shorter-wavelength fluctuations. The measured $k_\perp$ consists of radial, poloidal, and toroidal contributions, which vary with chord position. Far-forward collective scattering is expected to be more sensitive to density fluctuations than heterodyne interferometry, since only one mixer is required in its operation while the interferometry technique requires two mixers (additional one for reference).

III. EXPERIMENTAL MEASUREMENTS

As an example, Fig. 2(a) shows the spectrogram of scattered power from the chord positioned at the impact parameter x = 0.36 m. Due to the heterodyne detection scheme, two sidebands about the intermediate frequency (IF) f_0 (frequency offset between the probe and LO beam) appear. The strong peak $f - f_0 = 0$ is the un-scattered probe beam. The two symmetric sidebands ($f - f_0 > 0$ and $f - f_0 < 0$) result from the collection geometry where signals from scattered $\vec{k}_s = \vec{k}_0 \pm \vec{k}$ are viewed. Here, $\vec{k}$ is the wavevector of the plasma fluctuation and subscripts "s" and "o" refer to the scattered and incident electromagnetic (EM) waves, respectively. The $m = 1$, $n = 5$ tearing mode is clearly visible throughout the time window in the frequency range of 0–20 kHz. Here, m and n are poloidal and toroidal mode numbers, respectively. The tearing mode frequency (f) is dominated by a Doppler shift related to the toroidal flow ($f \sim k_\phi \upsilon_\phi / 2\pi$), where k_ϕ is the toroidal wavenumber and υ_ϕ is the toroidal flow. The dominant frequency measured by scattering tracks the tearing mode frequency as measured by the edge magnetic coils as seen in

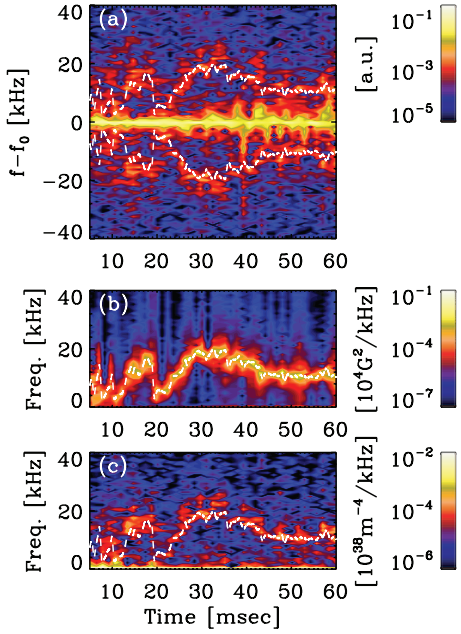

FIG. 2. Spectrogram of (a) far-forward scattering at R-R_0 = 0.36 m, (b) the (1,5) magnetic fluctuations by the edge magnetic coils, (c) density fluctuations from interferometry at R-R_0 = 0.36 m. The dashed line on the top of contour plot is the frequency of (1, 5) tearing mode from the edge magnetic coils.

Fig. 2(b). For the purpose of comparison, the spectrogram of line-integrated density fluctuations from the simultaneous operation of interferometry is shown in Fig. 2(c). The tearing mode is also clearly visible and the measured frequency also tracks well with those from the edge magnetic coils. The fluctuations below 5 kHz observed by interferometry tend to be cleaner than those on the collective scattering. This might be caused by the temporal variation of the IF frequency f_0 throughout the discharge, which broadens the contribution from the un-scattered beam in the frequency and reduces the sensitivity of the collective scattering to low-frequency fluctuations.

In addition to coherent tearing instabilities, broadband turbulence is also observed on the scattering signal. Figure 3 shows the spectra of density fluctuations for discharge conditions: plasma current 400 kA and central line-averaged density $1.0 \times 10^{19}\text{m}^{-3}$. To reduce the statistical noise, these spectra are averaged over 1000 events from similar plasma parameters and each event has a duration of 1.0 ms. Figure 3(a) is from the chord at R-R_0 = 0.36 m. The peak at 15 kHz corresponds to the (1,5) tearing mode as discussed previously. The noise is estimated from the data collected before plasma discharges. Broadband fluctuations are observed above the noise floor at frequencies up to 500 kHz. These broadband fluctuations exhibit a power law dependence on frequency, $P_s \propto f^{-3.3}$. Figure 3(b) is from the more core-localized chord at R-R_0 = 0.06 m. Here, the fluctuation level is reduced for both the coherent tearing mode and broadband fluctuations. The peak corresponding to the (1,5) tearing mode at 15 kHz is less pronounced. Furthermore, broadband fluctuations remain above the noise floor only up to 400 kHz. The index of the power law dependence on frequency also slightly changes, $P_s \propto f^{-3.0}$. The reference channel allows for the simultaneous

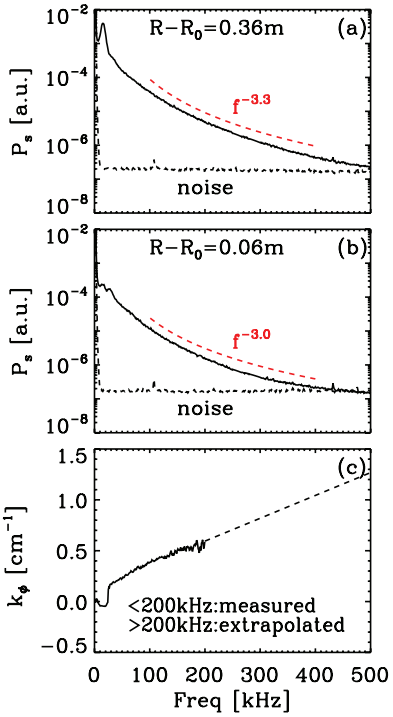

FIG. 3. Frequency spectrum of far-forward scattering at (a) R-R_0 = 0.36 m and (b) R-R_0 = 0.06 m, where the bottom dashed line is the noise floor estimated from the data before the discharge and the top dashed line is a best power-law fit of broadband fluctuations from 100 kHz to 400 kHz. (c) Toroidal wavenumber (k_ϕ), where the solid curve below 200 kHz is resolved by correlating two interferometry chords separated by 5° in the toroidal direction and the dashed line above 200 kHz is a linear extrapolation.

operation of the interferometry diagnostic. Two interferometry channels at R-R_0 = 0.36 m and 0.43 m are separated in the toroidal direction by 5°. The cross-phase between these two toroidally separated interferometry channels provides information on the toroidal wavenumber frequency dependence. As shown in Fig. 3(c), the toroidal wavenumber (k_ϕ) is resolved up to 200 kHz. The coherence between two interferometry channels drops below the noise floor above 200 kHz, indicating a lack of coherence for these fluctuations likely due to the radial chord spatial separation of ~7 cm. The toroidal wavenumber at 15 kHz is -0.04 cm^{-1}, roughly consistent with the toroidal mode $n = 5$ obtained from the magnetic coils. Above 40 kHz, the wavenumber shows a linear dependence on frequency. With the assumption that the linear dependence extends up to 500 kHz, the toroidal wavenumber at 500 kHz reaches ~1.2 cm^{-1}, which is near the maximum detectable $k_\perp \sim \pi/w$ limited by the beam width $w \sim 2.5$ cm.

Recently, a 1 MW 25 keV NBI became operational on MST with a tangency major radius of $R = 1.5$ in the direction of the plasma current.[14] With the application of NBI, a new instability has been observed in MST. This instability is likely driven by energetic particles. Figure 4 shows forward-scattering measurements in plasmas with and without NBI. The major plasma parameters are similar in these two types of plasmas, where the plasma current is 300 kA and central line-averaged density is 0.7×10^{19}m^{-3}. A coherent mode at about 90 kHz is observed in NBI-heated plasmas, as shown in Fig. 4. This coherent mode is absent in the plasma without NBI. In addition, in plasmas with NBI, the tearing mode

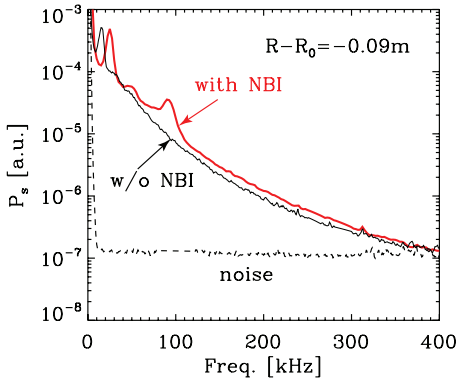

FIG. 4. Frequency spectrum of scattering power at R-$R_0 = -0.09$ m in plasmas with and without NBI, where the noise floor is estimated from the data before the discharge.

frequency is also upshifted from 15 kHz to 28 kHz, which is due to the external torque induced by co-injected NBI acting to increase the toroidal flow. An upshift of the broadband fluctuation is also observed.

IV. SUMMARY

Far-forward collective scattering is now operational on the MST-RFP. Initial measurements include global tearing mode, NBI-driven instabilities, and broadband fluctuations. Future plans involve upgrading the mixers to improve diagnostic sensitivity and optimizing the collecting optics to expand toward shorter-wavelength fluctuations. Measurements in high-performance RFP plasmas will be performed and comparison with numerical modeling will be attempted.

ACKNOWLEDGMENTS

The authors wish to thank the MST group for their contributions. This work is supported by U.S. Department of Energy.

[1]M. Greenwald, Phys. Plasmas **17**, 058101 (2010).
[2]J. S. Sarff, N. E. Lanier, S. C. Prager, and M. R. Stoneking, Phys. Rev. Lett. **78**, 62 (1997).
[3]D. F. Escande, R. Paccagnella, S. Cappello, C. Marchetto, and F. D'Angelo, Phys. Rev. Lett. **85**, 3169 (2000).
[4]W. F. Bergerson *et al.*, Phys. Rev. Lett. **107**, 255001 (2011).
[5]V. Tangri, P. W. Terry, and R. E. Waltz, Phys. Plasmas **18**, 052310 (2011).
[6]F. Sattin, X. Garbet, and S. C. Guo, Plasma Phys. Controlled Fusion **52**, 105002 (2010).
[7]I. Predebon, F. Sattin, M. Veranda, D. Bonfiglio, and S. Cappello, Phys. Rev. Lett. **105**, 195001 (2010).
[8]D. L. Brower, Y. Jiang, W. X. Ding, S. D. Terry, N. E. Lanier, J. K. Anderson, C. B. Forest, and D. Holly, Rev. Sci. Instrum. **72**, 1077 (2001).
[9]W. X. Ding, D. L. Brower, W. F. Bergerson, and L. Lin, Rev. Sci. Instrum. **81**, 10D508 (2010).
[10]R. N. Dexter, D. W. Kerst, T. W. Lovell, S. C. Prager, and J. C. Sprott, Fusion Technol. **19**, 131 (1991).
[11]D. E. Evans, E. J. Doyle, D. Frigione, M. von Hellermann, and A. Murdoch, Plasma Phys. **25**, 617 (1983).
[12]D. R. Smith, E. Mazzucato, W. Lee, H. K. Park, C. W. Domier, and N. C. Luhmann, Rev. Sci. Instrum. **79**, 123501 (2008).
[13]C. B. Deng and D. L. Brower, Rev. Sci. Instrum. **81**, 10D503 (2010).
[14]J. K. Anderson *et al.*, Trans. Fusion Sci. Technol. **59**, 27 (2011).